



ELSEVIER

Neurobiology of Aging xxx (2009) xxx–xxx

**NEUROBIOLOGY
OF
AGING**

www.elsevier.com/locate/neuaging

Brain regional lesion burden and impaired mobility in the elderly

Nicola Moscufo^{a,c,*}, Charles R.G. Guttmann^{a,b}, Dominik Meier^a, Istvan Csapo^a,
Peter G. Hildenbrand^{a,d}, Brian C. Healy^b, Julia A. Schmidt^c, Leslie Wolfson^c

^a Center for Neurological Imaging, Department of Radiology, Brigham and Women's Hospital, Harvard Medical School, Boston, MA 02115, USA

^b Department of Neurology, Brigham and Women's Hospital, Harvard Medical School, Boston, MA 02115, USA

^c Department of Neurology, University of Connecticut Health Center, Farmington, CT 06030, USA

^d Lahey Clinic, Burlington, MA 01805, USA

Received 17 November 2008; received in revised form 2 April 2009; accepted 12 April 2009

Abstract

This study investigated the relationship of brain white matter (WM) lesions affecting specific neural networks with decreased mobility in ninety-nine healthy community-dwelling subjects ≥ 75 years old prospectively enrolled by age and mobility status. We assessed lesion burden in the genu, body and splenium of corpus callosum; anterior, superior and posterior corona radiata; anterior and posterior limbs of internal capsule; corticospinal tract; and superior longitudinal fasciculus. Burden in the splenium of corpus callosum (SCC) demonstrated the highest correlation particularly with walking speed ($r=0.4$, $p<10^{-4}$), and in logistic regression it was the best regional predictor of low mobility performance. We also found that independent of mobility, corona radiata has the largest lesion burden with anterior (ACR) and posterior (PCR) aspects being the most frequently affected. The results suggest that compromised inter-hemispheric integration of visuospatial information through the SCC plays an important role in mobility impairment in the elderly. The relatively high lesion susceptibility of ACR and PCR in all subjects may obscure the importance of these lesions in mobility impairment.

© 2009 Elsevier Inc. All rights reserved.

Keywords: Aging; Mobility; Brain; White matter; White matter hyperintensity; Splenium of corpus callosum; Corona radiata; Magnetic resonance imaging

1. Introduction

Mobility impairment occurs in 14–50% of those between 65 and 85 years (Odenheimer et al., 1994) and has social and economic consequences as it is a cause of falls and dependence. While mobility impairment in the elderly is multifactorial, brain WM damage has been identified as one pathogenic mediator (Briley et al., 1997; Sachdev et al., 2005; Starr et al., 2003). Prevalence of WM hyperintensities (WMH) in healthy elderly ranges between 27 (Breteler et al., 1994) and 90% (de Leeuw et al., 2000) depending on the defining criteria. In addition to mobility impairment, WMH is also linked to cognitive decline (Charlton et al., 2006; Garde et al., 2000; Mungas et al., 2002; Prins et al.,

2005; van den Heuvel et al., 2006) and urinary dysfunction (Sakakibara et al., 1999). Data suggests an ischemic origin of the WMH (Pantoni and Garcia, 1997) with large studies, e.g., Framingham study (DeCarli et al., 2005), Rotterdam study (de Leeuw et al., 2001), Austrian Stroke prevention study (Schmidt et al., 1999, 2005) supporting the link of WMH to vascular disease (Ikram et al., 2006; Prins et al., 2005). Risk factors associated with WMH include hypertension (Dufouil et al., 2001) as well as metabolic factors, e.g., diabetes, homocysteine, hyperlipidemia, and C-reactive protein (Longstreth et al., 1996). Balance during standing conditions and dynamic movement relies on timely processing of vestibular, visual, and tactile-proprioceptive inputs to produce a coordinated motor response that maintains or restores body alignment with the base of support. Failure to rapidly compensate destabilizing forces results in poor balance and falls. Although for the majority of cases there are identifiable pathologies causing mobility impairment, e.g., CNS degenerative disease, arthritis, and deconditioning, for

* Corresponding author at: Center for Neurological Imaging, Brigham and Women's Hospital, 221 Longwood Avenue, RF-398, Boston, MA, USA. Tel.: +1 617 278 0185; fax: +1 617 264 5154.

E-mail address: moscufo@bwh.harvard.edu (N. Moscufo).

a significant fraction no link to a specific disease can be identified. Several cross-sectional studies on elderly subjects have demonstrated a relationship between brain WMH and lower extremity motor function (Masdeu et al., 1989; Baloh et al., 1995; Briley et al., 1997; Longstreth et al., 1996; Camicioli et al., 1999; Guttmann et al., 2000; Baezner et al., 2008). This relationship has been observed also in longitudinal analyses that showed worsening mobility to be associated with increasing WMH (Whitman et al., 2001; Baloh et al., 2003; Wolfson et al., 2005). However, the role/s and progression of regional brain WMH in mobility decline in the elderly population remain to be defined. We hypothesize that WM damage compromises areas of the brain required for sensorimotor integration underlying motor control. Accordingly, we will attempt to define the role of regional lesion burden in mobility impairment, utilizing a prospective study involving ninety-nine healthy old individuals stratified by age and mobility. We report here the results of the cross-sectional analysis on baseline mobility status with regional distribution of WMH. We assessed WM damage in areas containing motor control pathways (corticospinal tracts, internal capsule), mediating inter- and intra-hemispheric integration of visual and other sensory inputs (corpus callosum, superior longitudinal fasciculus), and periventricular regions containing afferent as well as efferent corticospinal connections (corona radiata), and characterized the association of these regional burdens with mobility performance.

2. Methods

2.1. Subjects

Ninety-nine community-dwelling subjects 75–90 years old were recruited for a 4-year prospective study defining the relationship between mobility impairment, brain changes, and cardiovascular risk factors. Subjects were recruited through multiple methods. Newspaper articles in the Hartford Courant and New Britain Herald generated the largest response, and were supplemented by presentations at senior centers, retirement communities, civic organizations and health fairs. Advertisements were placed in community newsletters, apartment buildings, and recruitment packets were sent to all Hartford faith-based organizations. A research volunteer database was utilized and geriatricians at the University of Connecticut Health Center were asked to refer patients. Exclusion criteria included: systemic conditions (e.g., severe arthritis) and neurologic disease (e.g., neuropathy, Parkinson's disease) compromising mobility, medication impairing motor function, cognitive impairment (Mini-Mental State Exam, MMSE <24), corrected distance vision >20/70, unstable cardiovascular disease (e.g., myocardial infarction within 6 months, unstable angina), pulmonary disease requiring oxygen, inability to walk 10 m independently in <50 s, lower extremity amputation, weight >114 kg, claus-

trophobia, pacemaker or other metallic devices/implants, excessive alcohol intake and expected lifespan <4 years. Phone screening was completed on 312 people. All eligible persons were invited to an orientation session and were fully informed and provided consent before further screening of medical history, MMSE and mobility. Of the 164 still eligible, 117 returned for a physical exam performed by the senior investigator (LW) who also administered the remaining exclusion criteria. Seventeen subjects were excluded due to exam findings, arthritis and claustrophobia, and one due to a clinically silent cerebellar meningioma found on MRI. To ensure study compliance MRIs were reviewed by an on-site radiologist and by a neuroradiologist (PGH) at the neuroimaging core. Study population images were carefully reviewed for co-morbidities including cerebral infarction, and intracranial mass lesions. Subjects were enrolled by age and mobility to fill a 3 × 3 stratification matrix (Table 1). The Institutional Review Boards of participating institutions approved the protocol.

2.2. Mobility assessment

Mobility was measured by one of the authors (JAS), using the short physical performance battery (SPPB) (Guralnik et al., 1994), which rates performance by comparison to a standardized sample with one point for each quartile (best = 4). SPPB is the summed performance on three components: standing balance (SB) during tandem, semi-tandem and side-by-side stance; five chair rises (CR); and time to walk 2.5 m (WS). We defined three categories of normal (SPPB = 11–12), mildly impaired (SPPB = 9–10) and moderately impaired (SPPB <9) mobility, hereafter called normal (SPPB: 11.3 ± 0.4; median: 11), intermediate (SPPB: 9.7 ± 0.4; median: 10), and impaired (SPPB: 6.6 ± 1.5; median: 6.5).

2.3. MR imaging

High-resolution MR images of the head were acquired at the Institute of Living (Hartford, Connecticut) using three MR sequences on a 3-Tesla Siemens Allegra scanner (Erlangen, Germany): T1-weighted Magnetization Prepared Rapid Gradient Echo (MPRAGE) (176 contiguous 1-mm thick axial slices, TR/TE = 2500/2.74 ms, TI = 900 ms, matrix size = 256 × 208, in-plane pixel spacing = 1 mm × 1 mm); 3D-Fast Spin Echo (T2) (176 contiguous 1-mm thick sagittal slices, TR/TE = 2500/353 ms, matrix size = 256 × 220, in-plane pixel spacing = 1 mm × 1 mm), and Fluid Attenuated Inversion Recovery (FLAIR) (128 contiguous 1.3-mm thick sagittal slices, TR/TE = 6000/353 ms, TI = 2200 ms, matrix size = 256 × 208, in-plane pixel spacing = 1 mm × 1 mm). Pre-processing included correction of magnetic field-related signal inhomogeneities (Sled et al., 1998) and linear affine registration of FLAIR and T2 series to the MPRAGE series (Jenkinson and Smith, 2001).

Table 1
Characteristics of study cohort.

	All (n = 99)	Mobility groups		
		Normal (n = 33)	Intermediate (n = 36)	Impaired (n = 30)
Subjects 75–79 years (F/M)	29 (16/13)	11 (6/5)	11 (6/5)	7 (4/3)
Subjects 80–84 years (F/M)	38 (24/14)	12 (8/4)	13 (8/5)	13 (8/5)
Subjects ≥85 years (F/M)	32 (17/15)	10 (5/5)	12 (6/6)	10 (6/4)
Age (years)	83 ± 4	82.0 ± 4.4	83.0 ± 3.9	83.3 ± 4.0
Sex (F/M)	57/42	19/14	20/16	18/12
MMSE	28.5 ± 1.3	28.7 ± 1.3	28.4 ± 1.4	28.3 ± 1.2
BMI	25.6 ± 3.9	24.3 ± 2.8^a	25.3 ± 3.1	27.4 ± 5.1
Subjects with hypertension	71 (71%)	22 (66%)	26 (72%)	23 (77%)
BPF	0.704 ± 0.034	0.714 ± 0.038^b	0.706 ± 0.034	0.692 ± 0.030
WMF	0.260 ± 0.057	0.270 ± 0.053^c	0.270 ± 0.045^d	0.235 ± 0.069
GMF	0.443 ± 0.051	0.442 ± 0.046	0.435 ± 0.047	0.455 ± 0.061
WMHF	0.010 ± 0.010	0.008 ± 0.008^e	0.009 ± 0.006	0.013 ± 0.012

Brain volumes are expressed as fraction of ICC (mean: 1395 ± 138 mL, range: 1132–1780 mL).

^a Significant difference with impaired group (Mann–Whitney): $p = 0.008$.

^b Significant difference with impaired group (Mann–Whitney): $p = 0.017$.

^c Significant difference with impaired group (Mann–Whitney): $p = 0.034$.

^d Significant difference with impaired group (Mann–Whitney): $p = 0.049$.

^e Significant difference with impaired group (Mann–Whitney): $p = 0.040$.

2.4. Intracranial cavity (ICC)

The ICC was obtained from the T2 series via semi-automated skull stripping using custom-made software implemented in Matlab (Mathworks Inc., Natick, Massachusetts). ICC included cortical cerebrospinal fluid and was used to exclude non-brain voxels from the subsequent tissue class segmentation.

2.5. Probabilistic brain atlas (ICBM)

During segmentation, ICBM brain atlas (International Consortium on Brain Mapping, UCLA) was warped to each subject's brain through linear affine registration (Jenkinson and Smith, 2001), followed by non-rigid registration as implemented in 3D-Slicer to provide a probabilistic template for gray matter (GM) and WM classification (Pohl et al., 2004). The ICBM was also used for stereotaxic analysis as standard space to which the brain of each subject was normalized.

2.6. Brain segmentation

MPRAGE and FLAIR images were used for semi-automated segmentation into WM, GM, WMH, and cerebrospinal fluid. Brain parenchymal fraction (BPF), an index of brain atrophy, was calculated as follows: sum of WM, GM, and WMH volumes divided by the total ICC volume. Similarly, to account for head size variability, individual tissue class volumes were also normalized and expressed as fraction of ICC (GMF, WMF, WMHF). WMHs were defined as WM areas that were hyper-intense in FLAIR images (Fig. 1A). To obtain the optimal segmentation we combined the outputs of three separate pipelines: single-channel and double-channel using 3D-Slicer (Pohl et al., 2004) and the

segmentation module of FreeSurfer (Fischl et al., 2002). True WMH had to be classified in at least two of the three segmentation outputs (>10% spatial overlap). WMH three pixels or less in size were excluded.

2.7. Regional WMH burden

We used the brain atlas ICBM DTI-81 (Mori et al., 2008) (called hereafter white matter parcellation atlas, WMPA) for automated WM parcellation and to subsequently mea-

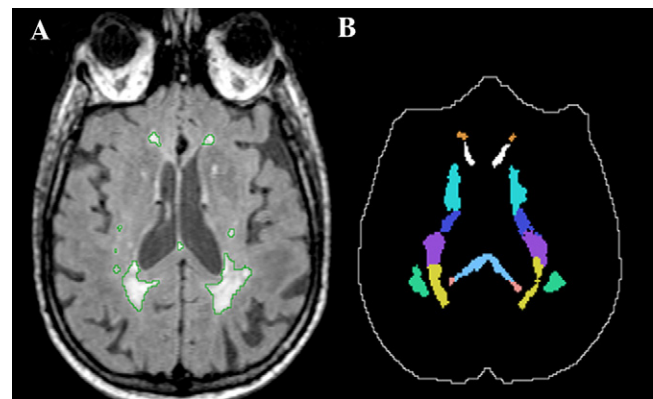


Fig. 1. Example illustrating some of the white matter ROIs analyzed in the study. Panel A shows a grayscale FLAIR image with the WMH outlined in green. Panel B shows the ROIs mask corresponding to panel A that we used for determining the regional WMH burden. In panel B the intracranial cavity mask is outlined in white. Solid colors in panel B (top to bottom): orange (anterior corona radiata, ACR), white (genu of the corpus callosum, GCC), green-blue (anterior limb of the internal capsule, ALIC), dark blue (posterior limb of the internal capsule, PLIC), purple (superior corona radiata, SCR), yellow (posterior corona radiata, PCR), light blue (body of the corpus callosum, BCC), pink (splenium of the corpus callosum, SCC), green (superior longitudinal fasciculus, SLF). (For interpretation of the references to color in this figure legend, the reader is referred to the web version of the article.)

sure lesion volumes within supratentorial regions of interest (ROIs). The WMPA was spatially normalized to each subject's brain (example in Fig. 1) using the linear and non-linear transforms from the ICBM registration (described above) preceded by a separate affine registration between the WMPA and ICBM. Cerebellum and brainstem were excluded since minimal or no WMH were detected by independent review of the MR scans by a neuroradiologist (PGH). The ROIs selected are genu, body and splenium of corpus callosum (GCC, BCC, SCC); corona radiata— anterior, superior and posterior portion (ACR, SCR, PCR); internal capsule— anterior and posterior limbs (ALIC, PLIC); corticospinal tract (CST); and superior longitudinal fasciculus (SLF). GCC contains commissural fibers connecting areas of frontal and pre-frontal cortex. BCC contain commissural fibers connecting pre-motor, motor and somatosensory areas. SCC is crossed by fibers connecting parietal, temporal and occipital cortex sensing body position, i.e., somatosensory and visual areas. CST contains efferent fibers originating in the motor, pre-motor, supplementary motor cortices and in parietal somatosensory cortex. ALIC and PLIC contain projection fibers, e.g., frontal corticothalamic (ALIC) and thalamo-cortical connections to motor, somatosensory, and parietal cortex plus corticospinal fibers (PLIC). ACR, SCR, and PCR contain the same projection fibers that form the internal capsule traveling to and from the cerebral cortex. SLF contains long association fibers connecting the frontal and pre-frontal cortices to mostly visual occipital cortex. Regional WMH burden is expressed as percent of the ROI volume.

2.8. WMH anatomical distribution

Individual WMH segmentation maps were registered to the ICBM brain as a common anatomical space to produce a 3D frequency distribution map where voxel value indicates percent of subjects with WMH in that voxel.

2.9. Statistical analysis

We used the SPSS application (SPSS Inc., Chicago, IL). Initially we assessed sample normality. We used the Wilcoxon test for paired sample comparisons, Chi-square test for group comparison of categorical variables, Mann–Whitney *U*-test for inter-group comparisons, Pearson and Spearman for parametric and nonparametric correlation analysis. A two-tailed level of $\alpha \leq 0.05$ was the significance threshold. In correlation tests that included 10 ROIs family-wise Bonferroni criterion was used to correct for multiple measurements and $\alpha \leq 0.005$ was the significance threshold. For logistic regression we assigned values 1, 2, and 3 to subjects in the normal, intermediate, and impaired groups, respectively. First, we tested individual variables in univariate logistic regression. Finally, significant variables were all entered in a multivariate forward stepwise selection procedure to determine the best predictor/s of mobility.

3. Results

3.1. Cohort characteristics

Table 1 shows the characteristics of the study cohort and mobility groups. The preponderance of female subjects represents an effort to enroll a cohort reflective of the 60:40 gender ratios in the population for this age group. Most subjects (71%) were hypertensive but differences among mobility groups were not significant (Pearson $\chi^2 = 0.782$, $p = 0.676$). BPF was lower in intermediate and impaired groups compared to normals, but the difference was significant only between normal and impaired. Reduction of WMF is the driving factor for this difference. Average WMHF increased in the low mobility groups but the difference was significant only between normal and impaired. Cohort mean WMHF was 1% of ICC (median: 0.7%) with WMH burden equally distributed in both hemispheres (Wilcoxon, $p > 0.05$). Total WMH burden correlated with WS and SPPB (Table 2). Spearman correlation analysis showed an association of BPF with CR score ($r = 0.228$, $p = 0.02$). Body mass index (BMI) was associated with SB score ($r = -0.225$, $p = 0.025$) and was significantly higher in the impaired compared to normal.

3.2. BPF and age

BPF correlated with age (Spearman $r = -0.39$, $p < 10^{-4}$) and decreased by 0.3% (C.I. 95%: 0.17–0.48) yearly, comparable to published values (Fox et al., 1999; Whitwell et al., 2007). Linear regression indicates that age explains nearly 15% of BPF variance in our cohort (Pearson $R^2 = 0.147$). Age correlated with WMHF (Spearman, $r = 0.247$, $p = 0.014$) but not with WMF or GMF.

3.3. Regional WMH burden

To determine if specific regions were preferentially affected by WMH burden in mobility-impaired elderly, we selected ROIs known to contain neural pathways involved in the processing of sensory information including visual and body position (BCC, SCC, SLF), and in the subsequent motor response (CST, PLIC) as well other ROIs. Table 2 shows the association between WMH burden in these ROIs and mobility scores. WMH burden in all ROIs shows significant association with WS with the exception of SLF. Burden in SCC, ALIC and PLIC associate with SPPB score. Burden in SCC shows the highest correlation and is the only regional burden associated with CR score, although WMH burden in the ALIC shows borderline significance (Table 2).

Table 3 shows the mean volumes of the ROIs and their percentage affected by WMH. Differences are significant for WMH burdens in all ROIs except for SLF between impaired and normal, with SCC showing the highest significance. Lesion burden in SCC, ACR, SCR, ALIC and PLIC are also significantly higher in the impaired compared to the intermediate group. Differences did not reach significance between

Table 2
Spearman correlation of global and regional WMH with mobility performance scores.

WMH burden	Total SPPB score rho (p)	WS score rho (p)	CR score rho (p)	SB score rho (p)
Total WMH	− 0.223 (0.027)	− 0.288 (0.004)	−0.191 (0.058)	−0.082 (0.422)
GCC-WMH	−0.266 (0.008)	− 0.299 (0.003)	−0.259 (0.01)	−0.076 (0.454)
BCC-WMH	−0.212 (0.035)	− 0.316 (0.001)	−0.209 (0.038)	0.005 (0.959)
SCC-WMH	− 0.391 (6×10^{-5})	− 0.426 (10^{-5})	− 0.345 (4×10^{-4})	−0.160 (0.114)
ACR-WMH	−0.247 (0.014)	− 0.296 (0.003)	−0.220 (0.029)	−0.119 (0.241)
SCR-WMH	−0.257 (0.010)	− 0.339 (0.001)	−0.246 (0.014)	−0.075 (0.460)
PCR-WMH	−0.216 (0.032)	− 0.279 (0.005)	−0.203 (0.044)	−0.016 (0.872)
ALIC-WMH	− 0.294 (0.003)	− 0.356 (0.0003)	−0.265 (0.008)	−0.110 (0.280)
PLIC-WMH	− 0.283 (0.004)	− 0.343 (0.001)	−0.247 (0.014)	−0.093 (0.360)
CST-WMH	−0.268 (0.007)	− 0.300 (0.003)	−0.238 (0.018)	−0.101 (0.320)
SLF-WMH	−0.157 (0.120)	−0.212 (0.035)	−0.208 (0.039)	0.033 (0.749)

Significant rho values are in bold, set at $\alpha \leq 0.05$ for total WMH and at $\alpha \leq 0.005$ for the 10 ROIs (Bonferroni correction for multiple comparisons). Amount of WMH in SCC showed strongest and most significant correlation, particularly with the walking speed (WS) score.

intermediate and normal groups likely due to a non-linear relationship between increasing WMH burden and SPPB change.

We used logistic regression to assess which variable/s best predicted mobility performance. No variable was significant when we tested normal versus intermediate grouping as outcome. Regional burden variables that were significant predictors when tested individually were SCC-WMH ($\chi^2 = 12.3$, $p = 0.0004$), ALIC-WMH ($\chi^2 = 9.1$, $p = 0.003$), PLIC-WMH ($\chi^2 = 8.5$, $p = 0.003$), GCC-WMH ($\chi^2 = 8.4$, $p = 0.004$), CST-WMH ($\chi^2 = 7.7$, $p = 0.005$), BCC-WMH ($\chi^2 = 7.0$, $p = 0.008$), SCR-WMH ($\chi^2 = 7.0$, $p = 0.02$), and ACR-WMH ($\chi^2 = 5.4$, $p = 0.02$) in outcome A (normal versus impaired); and SCC-WMH ($\chi^2 = 8.7$, $p = 0.003$), ALIC-WMH ($\chi^2 = 8.4$, $p = 0.004$), ACR-WMH ($\chi^2 = 8.0$, $p = 0.005$), GCC-WMH ($\chi^2 = 6.7$, $p = 0.010$), and CST-WMH ($\chi^2 = 6.2$, $p = 0.013$) in outcome B (intermediate versus impaired). When these variables were all included in multivariate regression only SCC-WMH remained in the models and explained 23 and 16% of the variance (Nagelkerke Pseudo- R^2) for outcomes A and B, respectively. Among other variables tested hypertension, gender, and age were not significant whereas significant predictors were BMI, BPF,

WMF, and WMHF in outcome A, and WMF and WMHF in outcome B. When included in multivariate regression BMI ($\chi^2 = 6.1$, $p = 0.013$), SCC-WMH ($\chi^2 = 5.1$, $p = 0.024$), and BPF ($\chi^2 = 3.9$, $p = 0.048$) remained significant in the model for outcome A and additively explained 39% of the variance. For outcome B, SCC-WMH remained the only predictor.

3.4. Corona radiata most affected by WMH

We used spatially normalized segmentation outputs to produce a voxel-based WMH distribution map for each mobility group (Fig. 2). Periventricular WM was most frequently affected. The fraction of subjects with WM damage in anatomically identical location/s reached the maximum frequency values of 54, 63 and 67% in the normal, intermediate, and impaired groups, respectively. In the impaired group (Fig. 2C) WMHs occur in deep WM in 20–30% of the subjects. The most relevant neural pathway in these areas, the SLF, showed no significant difference in WMH burden between mobility groups (Table 3). Overlaying WMPA on the WMH frequency maps shows that in each group the ACR and PCR are the areas where lesions occur with the highest

Table 3
Volumes and WMH burden of the ROIs.

ROI	Volume (mL)	Mobility groups		
		Normal (% WMH, n = 33)	Intermediate (% WMH, n = 36)	Impaired (% WMH, n = 30)
GCC	9.42 ± 1.82	3.66 ± 2.92 ^a	4.16 ± 2.61	7.07 ± 6.30
BCC	10.10 ± 2.17	2.44 ± 2.29 ^a	2.78 ± 3.08	5.00 ± 5.18
SCC	10.98 ± 2.36	1.50 ± 2.00 ^b	1.90 ± 2.30 ^c	4.20 ± 4.00
ACR	7.73 ± 3.70	10.50 ± 10.17 ^a	9.80 ± 7.73 ^a	18.07 ± 15.18
SCR	8.00 ± 2.86	7.05 ± 7.40 ^a	8.18 ± 10.80 ^a	14.72 ± 14.98
PCR	4.95 ± 1.57	14.20 ± 15.90 ^a	15.60 ± 13.80	21.40 ± 17.90
ALIC	6.92 ± 2.25	2.21 ± 2.11 ^c	2.42 ± 1.92 ^a	4.98 ± 5.17
PLIC	8.19 ± 2.33	1.90 ± 1.70 ^a	2.50 ± 4.30 ^a	4.10 ± 4.40
CST	5.50 ± 1.16	2.30 ± 2.20 ^a	2.60 ± 1.90	4.50 ± 3.90
SLF	6.13 ± 2.80	3.7 ± 6.80	4.10 ± 6.50	8.80 ± 14.30

^a Significant differences (Mann–Whitney) with the impaired group were observed at $p < 0.05$.

^b Significant differences (Mann–Whitney) with the impaired group were observed at $p < 0.001$.

^c Significant differences (Mann–Whitney) with the impaired group were observed at $p < 0.01$.

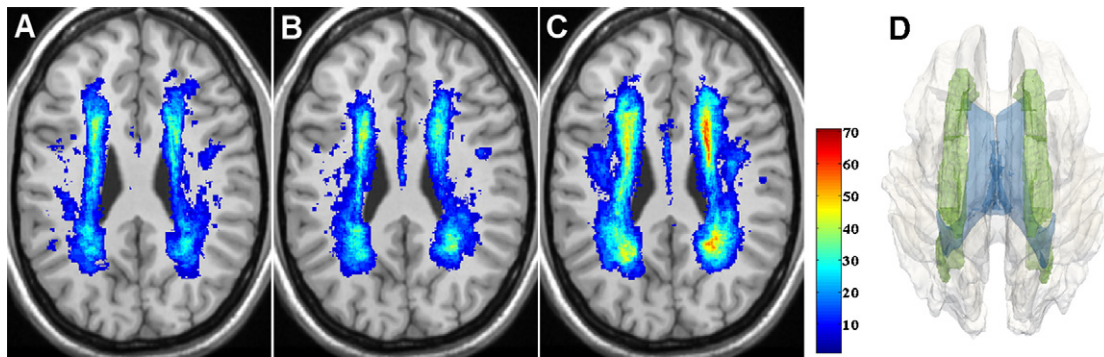


Fig. 2. Distribution and frequency of WMHs in the normal (A), intermediate (B), and impaired (C) mobility groups. WMH frequency maps are overlaid on the corresponding anatomical slice of the ICBM atlas. WMH frequency is color-coded in percent (color bar). Panel D shows a 3D model reconstruction of the most affected structure, the corona radiata (green), within the white matter (transparent gray), and with ventricles (blue) also shown. (For interpretation of the references to color in this figure legend, the reader is referred to the web version of the article.)

frequency. This is consistent with these regions also having the largest WMH fraction (Table 3).

4. Discussion

There are multiple risk factors for impaired mobility including age, hypertension, and WM lesions (Guttmann et al., 2000; Benson et al., 2002). Our study assessed hypertension as a risk factor but did not demonstrate that baseline blood pressure was linked to either total or regional WMH burden or mobility. This observation does not preclude hypertension as a risk factor, but rather suggests that its relative impact is reduced in our cohort of old subjects among whom hypertension is common. Although the preponderance of evidence suggests that hypertension is an important underlying factor in producing WM damage, the etiology of WMHs remains unclear and may be linked to multiple causes (Pantoni and Garcia, 1997). Abnormal permeability of the blood brain barrier within small vessels, with movement of proteinaceous fluid into surrounding tissue, is one alternative mechanism that can lead to WMHs (Wardlaw et al., 2003).

The finding that BMI is another significant predictor of mobility is not surprising as excess weight is a recognized factor associated with compromised mobility function as a result of biomechanical and deconditioning influences (LaCroix et al., 1993).

Our analysis assessed the lesion burden in anatomical areas containing motor control pathways as well as those involved in integrating visual and proprioceptive information. On average, WMH burden increased in all ROIs as mobility performance decreased indicating greater regional compromise of neural connectivity in the lower mobility groups, especially the impaired, compared to normal. This is consistent with an underlying patho-physiologic mechanism resulting in increasing damage to periventricular and deep WM with resultant functional impact.

Mobility impairment may occur in elderly individuals without comorbid physical conditions. Although the asso-

ciation between total brain WMH burden and diminished mobility is established, the role of the regional distribution of WMH is poorly understood. Baseline data from this longitudinal study of WMH and mobility demonstrated that lesion volume in the splenium of the corpus callosum has the strongest correlation and best regional predictive value for mobility, with higher specificity than other regional or even the global burden. This is consistent with previous observations (Benson et al., 2002). The SCC subserves inter-hemispheric visual and somatosensory transfer from occipital and posterior–inferior parietal cortices (Park et al., 2008) that are required for the integration of visual and spatial inputs to motor responses. Our results suggest that inefficient integration of inter-hemispheric visuospatial information due to WM damage is an important component of reduced mobility, particularly during walking.

Mobility requires integration of sensory inputs and motor outputs by multilevel motor control structures. Supra-spinal centers are important for initiation and adaptive control as they process feedback inputs from the limbs and guide movement in response to visual and vestibular inputs. In this study, we have used a reliable battery to assess lower extremity mobility functions relevant for daily living activities, i.e., walking, standing balance and chair rise, and found a significant correlation of WM lesion burden mainly with walking speed. The lack of association with standing balance and chair rise is consistent with the important role of the cerebellum in balance and that of strength in chair rise. By contrast, walking speed is reliant on complex multi-sensorial integration of the visual, vestibular, somatosensory systems through the cortex, basal ganglia and cerebellum. Dependence on multiple pathways might explain the association of reduced gait speed with most regional WMHs, particularly within the SCC.

The splenium of the corpus callosum may be specifically damaged in elderly and younger individuals (Conti et al., 2007) in other conditions, including arteriosclerotic encephalopathy (Uchino et al., 2006) and after radiation therapy (Pekala et al., 2003). In this study, there is no evidence of

preferential damage to the splenium since the WMHs here are not isolated and are associated with WMH burden in other regions. Furthermore, across mobility groups the SCC is the callosal region least affected by WMH in comparison with GCC and BCC. Therefore, we believe that WM lesions originate around the posterior horns of the ventricles and subsequently progress into the splenium.

At present, we can only speculate on the mechanism responsible for the observed association of lesion burden in this region with mobility impairment. Visuospatial and sensory integration through the splenium plays an important role in lower limbs function thereby making this area sensitive to lesions and to the associated reduced connectivity. The abundance of crossing thin fibers (Aboitiz et al., 1992) could increase this region's susceptibility to ischemic damage. Analyses that will include tractography on longitudinal data will test this interpretation.

Distribution and frequency maps confirmed the predominantly periventricular location of WMHs with the corona radiata being the most vulnerable area. The corona radiata is a fan-shaped fiber bundle containing connections of the sensory-motor cortex. This distribution is comparable to that observed in a previous study (Benson et al., 2002), which concluded that the frontal and parietal periventricular WMHs were associated with mobility impairment. A similar association in healthy elderly has been previously described (Camicioli et al., 1999; Silbert et al., 2008). It has been proposed that these periventricular areas are distal irrigation fields fed by end arterioles (Pantoni and Garcia, 1997) making them more susceptible to reduced cerebral perfusion and ischemia (Holland et al., 2008). The high WMH volume in the corona radiata in all groups of this study may obscure its importance in mobility impairment particularly if relationship is non-linear with a threshold. In addition, other age related non-motor dysfunctions that were not addressed in this study, e.g., urinary incontinence, cognitive or sensorial deficits, related to old age might result in progressive lesion burden in these areas.

We recognize three limitations of this study. The first is related to the possible sub-optimal alignment of WMPA to the brain of individual subjects. The advanced age of our cohort further complicated this problem due to age-related atrophy and ventricular enlargement. However, by using a two-step registration (linear followed by non-linear) we minimized the inevitable spatial mismatch. The second limitation is that cross-sectional analysis cannot establish a causal or temporal relationship due to lack of a direct link between WMH and mobility impairment. Our results are descriptive and represent an essential step for future longitudinal analyses on this cohort. We are also keenly aware of limitations in assessing mobility with SPPB, a widely used but relatively rudimentary test using ordinal measures. In addition, given the multifactorial nature of mobility impairment we cannot exclude the contribution of musculoskeletal, frailty and deconditioning factors. In our multivariate regression models we used a categorical variable derived from the SPPB

composite score, and we did not assess the contributions of individual sub-scores for balance, chair rise and gait speed. Although this is one approach to describe the study subject and to investigate the relationship between mobility and white matter lesion burden, other techniques could also have been applied, including a structural equation model. Such a model has the benefit of more fully exploring the relationships between the factors since they are all modeled simultaneously. We are investigating such models as part of future analyses.

We seek to develop MR-based diagnostic criteria for individuals at high risk of impaired mobility due to global or regional burden of WMH. The methodological approach we used in this study can also be a model for investigating other functions that are compromised during aging, e.g., cognition and incontinence.

In conclusion, our study identified the splenium of the corpus callosum as a potential anatomical and functional link between brain WM damage and impaired mobility observed in otherwise healthy elderly individuals. We also demonstrated a high prevalence of WMH lesion in the frontal and parietal parts of the corona radiata of all subjects, which may obscure the importance of these lesions in mobility impairment.

Abbreviations and acronyms

ACR	anterior corona radiata
ALIC	anterior limb of the internal capsule
BCC	body of the corpus callosum
BMI	body mass index
BPF	brain parenchyma fraction
CR	chair rise
CST	corticospinal tract
FLAIR	fluid attenuated inversion recovery
GCC	genu of the corpus callosum
GM	gray matter
GMF	gray matter fraction
ICC	intracranial cavity
ICBM	international consortium on brain mapping, UCLA
MMSE	mini-mental state exam
MPRAGE	magnetization prepared rapid gradient echo
MR	magnetic resonance
MRI	magnetic resonance imaging
PCR	posterior corona radiata
PLIC	posterior limb of the internal capsule
ROI	region of interest
SB	standing balance
SCC	splenium of the corpus callosum
SCR	superior corona radiata
SLF	superior longitudinal fasciculus
SPPB	short physical performance battery
TE	echo time
TI	inversion time
TR	repetition time
WM	white matter
WMF	white matter fraction

WMH white matter hyperintensity
 WMHF white matter hyperintensity fraction
 WMPA white matter parcellation atlas
 WS walking speed

Conflict of interest

The authors declare no conflict of interest.

Acknowledgments

Study supported by the National Institute on Aging - AG022092 (LW, CRGG); National Institute on Aging Training Grant - AG022092-01A1S1 (NM); University of Connecticut Health Center General Clinical Research Center Grant M01 RR06192; NIH 5 P41 RR13218.

We wish to thank Julie Raulukaitis and Dr. Godfrey Pearlson for their expertise in MR image acquisition, Antal Kucsai, Vince Calhoun, Dae Kim and Greg Book for their kind assistance with MR image transfer and processing, Charles B. Hall for advice on statistical analyses, Dorothy Wakefield for database assistance, Marek Kubicki for advice with the brain atlas, Yang Duang for expert neuroradiological assistance and Maria Liguori for insightful discussions.

References

- Aboitiz, F., Scheibel, A.B., Fisher, R.S., Zaidel, E., 1992. Fiber composition of the human corpus callosum. *Brain Res.* 598, 143–153.
- Baezner, H., Blahak, C., Poggesi, A., Pantoni, L., Inzitari, D., Chabriat, H., Erkinjuntti, T., Fazekas, F., Ferro, J.M., Langhorne, P., O'Brien, J., Scheltens, P., Visser, M.C., Wahlund, L.O., Waldemar, G., Wallin, A., Hennerici, M.G., 2008. Association of gait and balance disorders with age-related white matter changes: the LADIS study. *Neurology* 70, 935–942.
- Baloh, R.W., Yue, Q., Socotch, T.M., Jacobson, K.M., 1995. White matter lesions and disequilibrium in older people. I. Case–control comparison. *Arch. Neurol.* 52, 970–974.
- Baloh, R.W., Ying, S.H., Jacobson, K.M., 2003. A longitudinal study of gait and balance dysfunction in normal older people. *Arch. Neurol.* 60, 835–839.
- Benson, R.R., Guttmann, C.R., Wei, X., Warfield, S.K., Hall, C., Schmidt, J.A., Kikinis, R., Wolfson, L.I., 2002. Older people with impaired mobility have specific loci of periventricular abnormality on MRI. *Neurology* 58, 48–55.
- Breteler, M.M., van Swieten, J.C., Bots, M.L., Grobbee, D.E., Claus, J.J., van den Hout, J.H., van Harskamp, F., Tanghe, H.L., de Jong, P.T., van Gijn, J., Hofman, A., 1994. Cerebral white matter lesions, vascular risk factors, and cognitive function in a population-based study: the Rotterdam Study. *Neurology* 44, 1246–1252.
- Briley, D., Wasay, M., Sergent, S., Thomas, S., 1997. Cerebral white matter changes (leukoaraiosis), stroke, and gait disturbance. *J. Am. Geriatr. Soc.* 45, 1434–1438.
- Camicoli, R., Moore, M.M., Sexton, G., Howieson, D.B., Kaye, J.A., 1999. Age-related brain changes associated with motor function in healthy older people. *J. Am. Geriatr. Soc.* 47, 330–334.
- Charlton, R.A., Barrick, T.R., McIntyre, D.J., Shen, Y., O'Sullivan, M., Howe, F.A., Clark, C.A., Morris, R.G., Markus, H.S., 2006. White matter damage on diffusion tensor imaging correlates with age-related cognitive decline. *Neurology* 66, 217–222.
- Conti, M., Salis, A., Urigo, C., Canalis, L., Frau, S., Canalis, G.C., 2007. Transient focal lesion in the splenium of the corpus callosum: MR imaging with an attempt to clinical–physiopathological explanation and review of the literature. *Radiol. Med.* 112, 921–935.
- de Leeuw, F.E., de Groot, J.C., Breteler, M.M., 2000. White matter changes. Frequency and risk factors. In: Pantoni, L. (Ed.), *The Matter of White Matter*. Academic Pharmaceutical Productions, Utrecht, p. 19.
- de Leeuw, F.E., de Groot, J.C., Achten, E., Oudkerk, M., Ramos, L.M., Heijboer, R., Hofman, A., Jolles, J., van Gijn, J., Breteler, M.M., 2001. Prevalence of cerebral white matter lesions in elderly people: a population based magnetic resonance imaging study. *The Rotterdam Scan Study*. *J. Neurol. Neurosurg. Psychiatry* 70, 9–14.
- DeCarli, C., Massaro, J., Harvey, D., Hald, J., Tullberg, M., Au, R., Beiser, A., D'Agostino, R., Wolf, P.A., 2005. Measures of brain morphology and infarction in the framingham heart study: establishing what is normal. *Neurobiol. Aging* 26, 491–510.
- Dufouil, C., de Kersaint-Gilly, A., Besancon, V., Levy, C., Auffray, E., Brunereau, L., Alperovitch, A., Tzourio, C., 2001. Longitudinal study of blood pressure and white matter hyperintensities: the EVA MRI Cohort. *Neurology* 56, 921–926.
- Fischl, B., Salat, D.H., Busa, E., Albert, M., Dieterich, M., Haselgrove, C., van der Kouwe, A., Killiany, R., Kennedy, D., Klaveness, S., Montillo, A., Makris, N., Rosen, B., Dale, A.M., 2002. Whole brain segmentation: automated labeling of neuroanatomical structures in the human brain. *Neuron* 33, 341–355.
- Fox, N.C., Scahill, R.I., Crum, W.R., Rossor, M.N., 1999. Correlation between rates of brain atrophy and cognitive decline in AD. *Neurology* 52, 1687–1689.
- Garde, E., Mortensen, E.L., Krabbe, K., Rostrup, E., Larsson, H.B., 2000. Relation between age-related decline in intelligence and cerebral white-matter hyperintensities in healthy octogenarians: a longitudinal study. *Lancet* 356, 628–634.
- Guralnik, J.M., Simonsick, E.M., Ferrucci, L., Glynn, R.J., Berkman, L.F., Blazer, D.G., Scherr, P.A., Wallace, R.B., 1994. A short physical performance battery assessing lower extremity function: association with self-reported disability and prediction of mortality and nursing home admission. *J. Gerontol.* 49, M85–M94.
- Guttmann, C.R., Benson, R., Warfield, S.K., Wei, X., Anderson, M.C., Hall, C.B., Abu-Hasaballah, K., Mugler III, J.P., Wolfson, L., 2000. White matter abnormalities in mobility-impaired older persons. *Neurology* 54, 1277–1283.
- Holland, C.M., Smith, E.E., Csapo, I., Gurol, M.E., Brylka, D.A., Killiany, R.J., Blacker, D., Albert, M.S., Guttmann, C.R., Greenberg, S.M., 2008. Spatial distribution of white-matter hyperintensities in Alzheimer disease, cerebral amyloid angiopathy, and healthy aging. *Stroke* 39, 1127–1133.
- Ikram, M.K., De Jong, F.J., Van Dijk, E.J., Prins, N.D., Hofman, A., Breteler, M.M., De Jong, P.T., 2006. Retinal vessel diameters and cerebral small vessel disease: the Rotterdam Scan Study. *Brain* 129, 182–188.
- Jenkinson, M., Smith, S., 2001. A global optimisation method for robust affine registration of brain images. *Med. Image Anal.* 5, 143–156.
- LaCroix, A.Z., Guralnik, J.M., Berkman, L.F., Wallace, R.B., Satterfield, S., 1993. Maintaining mobility in late life. II. Smoking, alcohol consumption, physical activity, and body mass index. *Am. J. Epidemiol.* 137, 858–869.
- Longstreth Jr., W.T., Manolio, T.A., Arnold, A., Burke, G.L., Bryan, N., Jungreis, C.A., Enright, P.L., O'Leary, D., Fried, L., 1996. Clinical correlates of white matter findings on cranial magnetic resonance imaging of 3301 elderly people. *The Cardiovascular Health Study*. *Stroke* 27, 1274–1282.
- Masdeu, J.C., Wolfson, L., Lantos, G., Tobin, J.N., Grober, E., Whipple, R., Amerman, P., 1989. Brain white-matter changes in the elderly prone to falling. *Arch. Neurol.* 46, 1292–1296.
- Mori, S., Oishi, K., Jiang, H., Jiang, L., Li, X., Akhter, K., Hua, K., Faria, A.V., Mahmood, A., Woods, R., Toga, A.W., Pike, G.B., Neto, P.R.,

- Evans, A., Zhang, J., Huang, H., Miller, M.I., van Zijl, P., Mazziotta, J., 2008. Stereotaxic white matter atlas based on diffusion tensor imaging in an ICBM template. *Neuroimage* 40, 570–582.
- Mungas, D., Reed, B.R., Jagust, W.J., DeCarli, C., Mack, W.J., Kramer, J.H., Weiner, M.W., Schuff, N., Chui, H.C., 2002. Volumetric MRI predicts rate of cognitive decline related to AD and cerebrovascular disease. *Neurology* 59, 867–873.
- Odenheimer, G., Funkenstein, H.H., Beckett, L., Chown, M., Pilgrim, D., Evans, D., Albert, M., 1994. Comparison of neurologic changes in 'successfully aging' persons vs. the total aging population. *Arch. Neurol.* 51, 573–580.
- Pantoni, L., Garcia, J.H., 1997. Pathogenesis of leukoaraiosis: a review. *Stroke* 28, 652–659.
- Park, H.J., Kim, J.J., Lee, S.K., Seok, J.H., Chun, J., Kim, D.I., Lee, J.D., 2008. Corpus callosal connection mapping using cortical gray matter parcellation and DT-MRI. *Hum. Brain Mapp.* 29, 503–516.
- Pekala, J.S., Mamourian, A.C., Wishart, H.A., Hickey, W.F., Raque, J.D., 2003. Focal lesion in the splenium of the corpus callosum on FLAIR MR images: a common finding with aging and after brain radiation therapy. *Am. J. Neuroradiol.* 24, 855–861.
- Pohl, K.M., Bouix, S., Kikinis, R., Grimson, W.E.L., 2004. Anatomical guided segmentation with non-stationary tissue class distributions in an expectation-maximization framework. In: *IEEE International Symposium on Biomedical Imaging: From Nano to Macro*, Arlington, VA, USA, pp. 81–84.
- Prins, N.D., van Dijk, E.J., den Heijer, T., Vermeer, S.E., Jolles, J., Koudstaal, P.J., Hofman, A., Breteler, M.M., 2005. Cerebral small-vessel disease and decline in information processing speed, executive function and memory. *Brain* 128, 2034–2041.
- Sachdev, P.S., Wen, W., Christensen, H., Jorm, A.F., 2005. White matter hyperintensities are related to physical disability and poor motor function. *J. Neurol. Neurosurg. Psychiatry* 76, 362–367.
- Sakakibara, R., Hattori, T., Uchiyama, T., Yamanishi, T., 1999. Urinary function in elderly people with and without leukoaraiosis: relation to cognitive and gait function. *J. Neurol. Neurosurg. Psychiatry* 67, 658–660.
- Schmidt, R., Fazekas, F., Kapeller, P., Schmidt, H., Hartung, H.P., 1999. MRI white matter hyperintensities: three-year follow-up of the Austrian Stroke Prevention Study. *Neurology* 53, 132–139.
- Schmidt, R., Ropele, S., Enzinger, C., Petrovic, K., Smith, S., Schmidt, H., Matthews, P.M., Fazekas, F., 2005. White matter lesion progression, brain atrophy, and cognitive decline: the Austrian stroke prevention study. *Ann. Neurol.* 58, 610–616.
- Silbert, L.C., Nelson, C., Howieson, D.B., Moore, M.M., Kaye, J.A., 2008. Impact of white matter hyperintensity volume progression on rate of cognitive and motor decline. *Neurology* 71, 108–113.
- Sled, J.G., Zijdenbos, A.P., Evans, A.C., 1998. A nonparametric method for automatic correction of intensity nonuniformity in MRI data. *IEEE Trans. Med. Imaging* 17, 87–97.
- Starr, J.M., Leaper, S.A., Murray, A.D., Lemmon, H.A., Staff, R.T., Deary, I.J., Whalley, L.J., 2003. Brain white matter lesions detected by magnetic resonance [correction of resonance] imaging are associated with balance and gait speed. *J. Neurol. Neurosurg. Psychiatry* 74, 94–98.
- Uchino, A., Takase, Y., Nomiyama, K., Egashira, R., Kudo, S., 2006. Acquired lesions of the corpus callosum: MR imaging. *Eur. Radiol.* 16, 905–914.
- van den Heuvel, D.M., ten Dam, V.H., de Craen, A.J., Admiraal-Behloul, F., Olofsen, H., Bollen, E.L., Jolles, J., Murray, H.M., Blauw, G.J., Westendorp, R.G., van Buchem, M.A., 2006. Increase in periventricular white matter hyperintensities parallels decline in mental processing speed in a non-demented elderly population. *J. Neurol. Neurosurg. Psychiatry* 77, 149–153.
- Wardlaw, J.M., Sandercock, P.A.G., Dennis, M.S., Starr, J.M., 2003. Is breakdown of the blood–brain barrier responsible for lacunar stroke, leukoaraiosis and dementia? *Stroke* 34, 806–812.
- Whitman, G.T., Tang, Y., Lin, A., Baloh, R.W., 2001. A prospective study of cerebral white matter abnormalities in older people with gait dysfunction. *Neurology* 57, 990–994.
- Whitwell, J.L., Jack Jr., C.R., Parisi, J.E., Knopman, D.S., Boeve, B.F., Petersen, R.C., Ferman, T.J., Dickson, D.W., Josephs, K.A., 2007. Rates of cerebral atrophy differ in different degenerative pathologies. *Brain* 130, 1148–1158.
- Wolfson, L., Wei, X., Hall, C.B., Panzer, V., Wakefield, D., Benson, R.R., Schmidt, J.A., Warfield, S.K., Guttman, C.R., 2005. Accrual of MRI white matter abnormalities in elderly with normal and impaired mobility. *J. Neurol. Sci.* 232, 23–27.